Nagy, M., & Ribet, A. M. (1977) *Eur. J. Biochem. 77*, 77–85.
Nakagawa, S., Honda, S., Hasegawa, R., & Kobayashi, M. (1976) *Nihon Univ. J. Med. 18*, 55–63.
Salerno, C., & Giacomello, A. (1981) *J. Biol. Chem. 256*, 3671–3673.
Smithers, G. W., & O'Sullivan, W. J. (1982) *J. Biol. Chem. 257*, 6164–6170.
Thompson, R. E., Li, E. L., Spivey, H. O., Chandler, J. P., Katz, A. J., & Appleman, J. R. (1978) *Bioinorg. Chem. 9*, 35–45.
Vasquez, B., & Bieber, A. L. (1978) *Anal. Biochem. 84*, 504–511.
Victor, J., Leo-Mensah, A., & Sloan, D. L. (1979) *Biochemistry 18*, 3597–3604.

Active Site Cobalt(II)-Substituted Liver Alcohol Dehydrogenase: Characterization of Intermediates in the Reduction of *p*-Nitrobenzaldehyde by Rapid-Scanning Ultraviolet–Visible Spectroscopy†

Steven C. Koerber,‡ Alastair K. H. MacGibbon,§ Helmut Dietrich,⊥ Michael Zeppezauer, and Michael F. Dunn*

ABSTRACT: A detailed mechanistic investigation of the effects of Co(II) substitution for Zn(II) at the catalytic site of horse liver alcohol dehydrogenase (LADH) during the reduction of *p*-nitrobenzaldehyde (NBZA) by NADH using UV–visible rapid-scanning spectroscopy and stopped-flow rapid-mixing techniques is presented. Reaction was limited to a single turnover of sites by inclusion of pyrazole (pyr) to trap and inactivate the enzyme via formation of the E(NAD–pyr) adduct. The changes in the d–d and charge-transfer bands of the active site cobalt and the changes in the spectral bands of NADH and the E(NAD–pyr) adduct were studied via rapid scanning. The reaction to form the Co(II)E(NAD–pyr) complex and *p*-nitrobenzyl alcohol (NBZOH) was observed to occur in two distinct kinetic processes with apparent rate constants of 150–200 s^{-1} and 0.08 s^{-1} at pH 8.38. The time-resolved spectra and difference spectra established that NADH oxidation occurs in the first phase. Kinetic studies showed that in the first phase the oxidation of enzyme-bound NADH is preceded by at least two, rapid, preequilibrium processes: the first is presumed to be the binding of NBZA; the second is proposed to be a relaxation of the ternary Co(II)E(NADH, NBZA) complex involving NADH activation and/or an obligatory enzyme conformation change. Deuterium kinetic isotope experiments establish that hydride transfer does not limit the oxidation of NADH. On the basis of spectral comparisons, the product formed in the second phase is identified as the Co(II)E(NAD–pyr) complex. Analyses of the time-resolved spectra and difference spectra and comparisons with stable ternary complexes provide strong evidence indicating that the rate of formation of the Co(II)E(NAD–pyr) complex is limited by the dissociation of NBZOH from the Co(II)E(NAD^+, NBZOH) complex. The overall reaction time course was found to be significantly different from the time course observed for the native Zn(II) enzyme [Koerber, S. C., & Dunn, M. F. (1981) *Biochimie 63*, 97–102]. Although the microscopic origins for the different behaviors of the Co(II) and Zn(II) enzymes have not been determined, it is clear that substitution of Co(II) for Zn(II) substantially alters the mechanism of NBZA reduction by LADH.

The specific replacement of the active site zinc ion in horse liver alcohol dehydrogenase (LADH)[1] by other divalent metal ions is of considerable theoretical and experimental interest. The difficult task of replacement has been accomplished by several groups with varying degrees of success (Sloan et al., 1975; Shore & Santiago, 1975; Sytkowski & Vallee, 1978; Maret et al., 1979). However, the demonstration by Zeppezauer and co-workers (Maret et al., 1979) that the catalytic zinc ion can be specifically removed from the crystalline enzyme (Tilander et al., 1965) without changing the content of noncatalytic zinc and that the catalytic activity can be reconstituted in the crystalline state with other divalent metal ions resolves much ambiguity arising from previous reports.

This report is one of a series from our laboratories detailing mechanistic investigations of the reactions of specifically substituted Co(II)E(NADH) with aromatic aldehyde substrates. Cobalt substitution for zinc at the active site gives a chromophoric probe (Dietrich et al., 1979; Dunn et al., 1982) of the state of the metal ion along the reaction pathway. Since only the active site metal ion has been replaced, changes in observed kinetics with Co(II)E vis-à-vis native enzyme are presumed to reflect subtle changes in the chemistry and structure of the active site. Further, it is presumed that the

† From the Department of Biochemistry, University of California, Riverside, California 92521 (S.C.K., A.K.H.M., and M.F.D.), and the Fachbereich Analytische und Biologische Chemie, Universität des Saarlandes, Saarbrücken, FRG (H.D. and M.Z.). *Received November 9, 1982.* This work was supported by National Science Foundation Grants PCM 79-11526 and PCM 8108862, Grant Ze 152/7 of the Deutsche Forschungsgemeinschaft, and the Fonds der Chemischen Industrie. Portions of these studies were performed by S.C.K. and H.D. in partial satisfaction of requirements for the degree of Doctor of Philosophy.

‡ Present address: Molecular Biology Division, Veterans Administration Medical Center, San Francisco, CA 94121.
§ Present address: Department of Chemistry, Biochemistry and Biophysics, Massey University, Palmerston North, New Zealand.
⊥ Present address: Institut für Weinchemie and Getränketechnologie, Forschungsanstalt Geisenheim, 6222 Geisenheim, West Germany.

[1] Abbreviations: E, LADH, horse liver alcohol dehydrogenase; Co(II)E, Zn(II)E, Cd(II)E, and Ni(II)E, specific active site substituted alcohol dehydrogenase species; NAD^+ and NADH, respectively oxidized and reduced nicotinamide adenine dinucleotides; DACA, *trans*-4-(dimethylamino)cinnamaldehyde; NBZA and NBZOH, respectively *p*-nitrobenzaldehyde and *p*-nitrobenzyl alcohol; TFE, 2,2,2-trifluoroethanol; pyr, pyrazole; Tes, 2-[[tris(hydroxymethyl)methyl]amino]ethanesulfonic acid.

0006-2960/83/0422-3424$01.50/0

constraints imposed by protein tertiary structure (i.e., coordination number, geometry, and alignment of reacting species) ensure highly similar transition states for native and Co(II)-substituted enzyme, allowing a more detailed investigation of the role of the metal ion and the nature of the hydride transfer transition state in catalysis.

We report here the single turnover reaction of *p*-nitrobenzaldehyde (NBZA) with Co(II)E(NADH), studied via both rapid-scanning and single-wavelength UV–visible spectroscopy in combination with the rapid-mixing stopped-flow apparatus. Reactions were limited to a single turnover of sites by the inclusion of pyrazole in the reaction mixture. Pyrazole (pyr) is a potent inhibitor which reacts rapidly with the E(NAD^+) complex to form an E(NAD–pyr) adduct (McFarland & Bernhard, 1972; Dunn et al., 1979; Eklund et al., 1982). In these experiments pyr traps the E(NAD^+) complex during the course of the first turnover as dissociation of alcohol from the E(NAD^+, P) complex occurs. Because the Co(II)-E–NADH system contains multiple electronic transitions in the 300–700-nm region consisting of ligand-to-metal charge-transfer bands, d–d transitions, and the long wavelength band of the 1,4-dihydronicotinamide chromophore, the time-resolved spectra obtained during a single turnover contain a wealth of information relevant to the reaction mechanism. As will be shown, the reduction of NBZA by Co(II)E-bound NADH in the presence of pyrazole consists of a single, observable phase. This process is followed by a much slower phase during which product alcohol dissociates from the site and the Co(II)E-(NAD–pyr) adduct is formed.

Experimental Procedures

Materials

Buffer solutions were prepared from reagent-grade crystalline salts by using doubly glass-distilled water. With the exception of the 0.1 M Tes–0.15 M sodium chloride buffer, all buffers were kept free of chloride ion to minimize interference with coenzyme binding (Sund & Theorell, 1963). The coenzyme NAD^+ (Sigma Chemical Co., grade V) was used without further purification. For the kinetic isotope effect studies, both (4*R*)-4-deuterionicotinamide adenine dinucleotide (NADD) and isotopically normal NADH were synthesized by the method of Rafter & Colwick (1957) as modified by the method of Dunn & Hutchison (1973). The crude products were further purified by the method of Silverstein (1965). The reagents NBZA and pyrazole were purified by vacuum sublimation immediately prior to use.

Active site substituted cobalt LADH was prepared by the method of Maret et al. (1979). This procedure entails diffusion of cobaltous ion into crystalline enzyme which has been depleted of active site zinc ion (hereforth referred to as apoenzyme) via dialysis in the presence of 2,6-dipicolinic acid. All preparation, transport, storage, and manipulation of the apoenzyme and Co(II)-substituted enzyme were under water-saturated nitrogen to protect against oxidative degradation. The substituted enzyme crystals were dissolved in 0.2 M Tes–0.15 M sodium chloride buffer (pH 7.1); chloride ion was required for complete dissolution. From this concentrated stock, enzyme solutions were prepared by dilution with 4.5 mM Tes buffer (pH 7.15). Active site concentrations of stock enzyme solutions were determined spectrophotometrically (Maret et al., 1979; Dunn et al., 1982), and the preparation used in this study was found to have 79% active site occupancy relative to total protein; the remaining active sites appeared to contain no metal ion. Concentration conditions given in the text refer to the concentration of catalytically functional Co(II)-substituted enzyme sites expressed as normality (N).

Methods

Kinetic and Static Spectral Measurements. Routine UV–visible spectral and kinetic data were obtained with Varian 635, Cary 118C, and Hewlett-Packard 8450A spectrophotometers. Single wavelength transient kinetic studies were performed with a Durrum Model D-110 stopped-flow spectrophotometer (20-mm light path; dead time ca. 3.0 ms) interfaced for on-line computer data acquisition and analysis. The hardware and software for this system have been described (Dunn et al., 1979). The concentrations reported refer to conditions after mixing.

Rapid-Scanning Stopped-Flow (RSSF) Spectrophotometry. The RSSF spectrophotometer used in these studies is a hybrid system employing elements of the Durrum D-110 Kel-F flow and illumination systems with the Princeton Applied Research (PAR) OMA-2 multichannel analyzer, 1218 controller, and 1412 photodiode array detector together with an external time-delay firing circuit to ensure simultaneity of flow stoppage and data acquisition (Koerber, 1981).

The stopped-flow spectrophotometer was modified with a Durrum U4 white light bypass to allow cuvette illumination with the full spectral output of either a xenon or tungsten–iodide source for studies in the 300–450 or 450–700 nm ranges, respectively. Schott Glass filters, BG24 (300–450 nm) or GG400 (450–700 nm), were used to filter or attenuate unwanted light. Light exiting from the cuvette is focused via a spherical first-surface quartz mirror on the entrance of a J-Y polychromator equipped with a grating blazed at 240 nm. For the herein reported spectra, the repetitive scan rate is 16.48 ms/scan with scan delays introduced to give a pattern of scans corresponding to the time course of the observed kinetic phases (see Figures 2–5). Pixels were grouped in pairs with the signal from each pair summed and averaged.

In a typical experiment, a signal-averaged "100% transmission" reference spectrum (defined as the light transmitted by the buffer solution used) and the diode "dark current" spectrum are first collected and stored. By use of these reference spectra, the rapid-scanning data are converted to absorbance and stored directly on disk in a single operation. Some difference spectra were calculated and smoothed by using the method of Savitzsky & Golay (1964).

Results

Effects of Liganding on the Spectral Properties of the Co(II)-Substituted Enzyme. The static spectra of various binary and ternary complexes of Co(II)LADH are given in parts A and C and parts B and D of Figure 1 for the regions 300–440 and 440–700 nm, respectively. The spectra of substrate, *p*-nitrobenzaldehyde (NBZA), and product, *p*-nitrobenzyl alcohol (NBZOH), are included in Figure 1A for reference. The A and B designations refer to complexes with NADH, and the C and D designations refer to complexes with NAD^+. The different ordinate scale factors for the two wavelength regions reflect inherent differences in the magnitudes of the absorbencies in these regions. The Co(II)E spectrum (Figure 1A) is characterized by an intense charge-transfer band at 350 nm (ϵ = 7000 M^{-1} cm^{-1}, based on an 80 000-dalton dimer). The position and intensity of this band is shifted upon the formation of binary or ternary complexes. Due to the overlapping spectral bands of the NADH and Co(II) chromophores, the spectrum of the Co(II)E–(NADH, IBA) complex in the 300–350-nm region (Figure 1A) is complicated. Note that NBZA and NBZOH do not absorb in the visible region.

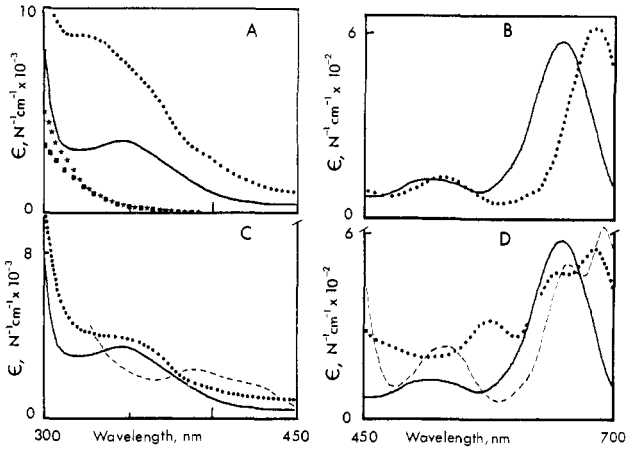

FIGURE 1: Comparison of the effects of the inhibitors isobutyramide (IBA), 2,2,2-trifluoroethanol (TFE), pyrazole (pyr) and coenzyme oxidation state on the UV–visible spectrum of Co(II)-substituted liver alcohol dehydrogenase. (A and B) The spectra of Co(II)E (—) and Co(II)E(NADH, IBA) (···). (C and D) The spectra of Co(II)E (—), Co(II)E(NAD^+, TFE) (···), and Co(II)E(NAD–pyr) (- - -). The spectra of *p*-nitrobenzaldehyde (NBZA) (■) and *p*-nitrobenzyl alcohol (NBZOH) (★) in 50 mM sodium pyrophosphate buffer, pH 8.75 and 25.0 ± 0.2 °C, are shown in (A) for comparison. The concentration of enzyme determined as Co(II)-substituted sites was 42.7 μN throughout. The spectra of the complexes were measured in separate experiments by using the following final concentrations of ligands: [NADH] = 41.2 μM; [IBA] = 90 mM; [NAD^+] = 490 μM; [TFE] = 125 mM; [pyr] = 20 mM; 25 mM Tes buffer, pH 7.0 and 25.0 ± 0.2 °C.

The presence of pyrazole in a binary complex with the Co(II) enzyme red shifts the 350-nm band to 365 nm and increases the intensity in the region 360–430 nm (data not shown). The adduct formed with NAD^+ and pyrazole further red shifts and splits this band giving new bands at ~400 and ~420 nm (Figure 1C). Hence, the region 395–450 nm is diagnostic for the formation of the Co(II)E(NAD–pyr) adduct, and this region is uncomplicated by other enzyme or coenzyme absorbancies.

In the region 500–600 nm, small intensity and λ_{max} differences obtain between enzyme and the binary complexes with either coenzyme form. The low intensity peak at 525 nm present in the spectra of both the Co(II) enzyme and the Co(II)E(NADH) complex is broadened and slightly intensified in the Co(II)E(NAD^+) complex (Dietrich & Zeppezauer, 1982). Further changes accompany the formation of ternary complexes with either neutral or anionic ligands (Figure 1B,C). The 525-nm bands observed for both the Co(II)E(NADH, IBA) and the Co(II)E(NAD–pyr) complexes shift to 575 nm upon the formation of the Co(II)E(NAD^+, TFE) complex or the Co(II)E(NAD^+, acetate) complex (spectrum not shown). This shift is presumed to reflect a lowering of the electronic transition energy via Coulombic interactions.

Marked changes in the 600–700-nm region accompany binary and ternary complex formation. The 650-nm band which characterizes the Co(II)E spectrum is red shifted to ca. 670 nm upon binding either NAD^+ or NADH (Maret et al., 1979). Note the presence of a very slight shoulder on the lower wavelength side of the 650-nm band in the spectrum of the Co(II)E(NADH, IBA) complex (Figure 1B). This shoulder does not appear in the spectrum of the Co(II)E(NAD^+) complex.

The most dramatic changes in the 600–700-nm region accompany the formation of ternary complexes. The spectra of the E(NAD^+, TFE) and E(NAD–pyr) complexes both show a red shifting and splitting of the enzyme 650-nm band, yielding peaks at ca. 650 and 670 nm (Figure 1D). The spectrum of the E(NAD^+, acetate) complex shows only a shift to ca. 675 nm (spectrum not shown).

Rapid-Scan Studies. It has been found that the UV and visible regions are better explored separately with the present instrumentation (see Experimental Procedures). A xenon lamp was needed to provide sufficient light intensity at low wavelengths; a tungsten lamp was used as a source for the longer wavelength region. Note that the absorbance changes in the UV region are roughly an order of magnitude larger than those in the visible region.

Parts A and B of Figure 2 show the rapid-scan spectral changes which occur in the UV and in the visible regions, respectively, upon mixing Co(II)E with NADH, NBZA, and pyr (experimental conditions are given in the caption). The family of time-resolved spectra for the wavelength range 300–450 nm (Figure 2A) shows decreasing optical densities in the region between 324 and 380 nm, viz., subsets b and c. In the regions 300–324 and 380–450 nm, the optical densities first decrease (spectra 1–7, the first 203 ms) and then increase (spectra 7–19, 203 ms–47.5 s). At 312 nm and at 398 nm, the initial and final optical densities are identical, whereas at 324 nm and at 380 nm, the optical density decreases during the first seven spectra and then remains constant throughout the remaining spectra. The final spectrum corresponds to completion of a single turnover of enzyme sites with the production of stoichiometric amounts of NBZOH and the Co(II)E(NAD–pyr) adduct. (Compare spectrum 19 of Figure 2A with the spectrum presented in Figure 1C.) Note that the increase in absorbance in the 300-nm region very likely is due to adduct formation between pyr and bound NAD^+ and to the production of NBZOH.

The family of spectra for the 450–750-nm wavelength range (Figure 2B) is more complex. Each spectrum in set a exhibits at least three, well-defined spectral bands. The subset of spectra in part b of Figure 2B shows the rapid formation of a new spectral band with $\lambda_{max} \simeq 575$ nm (spectra 1–7). This band then slowly decays away with concomitant formation of a band with λ_{max} ~530 nm, viz., spectra 7–19 in part c. During this slow phase, the band with $\lambda_{max} \simeq 680$ increases. Since NBZA, NBZOH, and NADH do not absorb in the 450–750-nm region of the spectrum, these traces record only the changes in the d–d transitions due to changes in ligation during a single turnover. The final trace (19) is the spectrum of the Co(II)E(NAD–pyr) complex (compare with the spectrum presented in Figure 1D).

From single-wavelength time slices at 324, 350, 398, and 575 nm (Figure 3), two distinct phases can be inferred in the transient spectra (Figure 2): a fast process (with $k_{obsd} \simeq 18$ s^{-1} under these conditions) and a very slow process (with $k_{obsd} \simeq 0.08$ s^{-1}), which (as will be shown) is the production of a Co(II)E(NAD–pyr) adduct.

Due to the large differences in the rates of the two observed processes (viz., Figure 3), it is possible to deconvolute the absorption changes via difference spectroscopy. Figure 4A compares the difference spectra for the fast phase, calculated by subtracting spectrum 7 of Figure 2A from spectra 1–6 (the time interval 0–203 ms). Note in Figure 4A that the position of the maximum for the set of difference spectra, ~336 nm, is nearly invariant during the fast phase. We assign this spectral change to the disappearance of bound NADH together with a concomitant shift and/or decrease in the intensity of the Co(II)E charge-transfer band. The difference spectra in Figure 4B were calculated by subtracting spectrum 19 of Figure 2A from spectra 7–18. These spectra are characterized by apparent isosbestic points at 324 and 380 nm, minima at

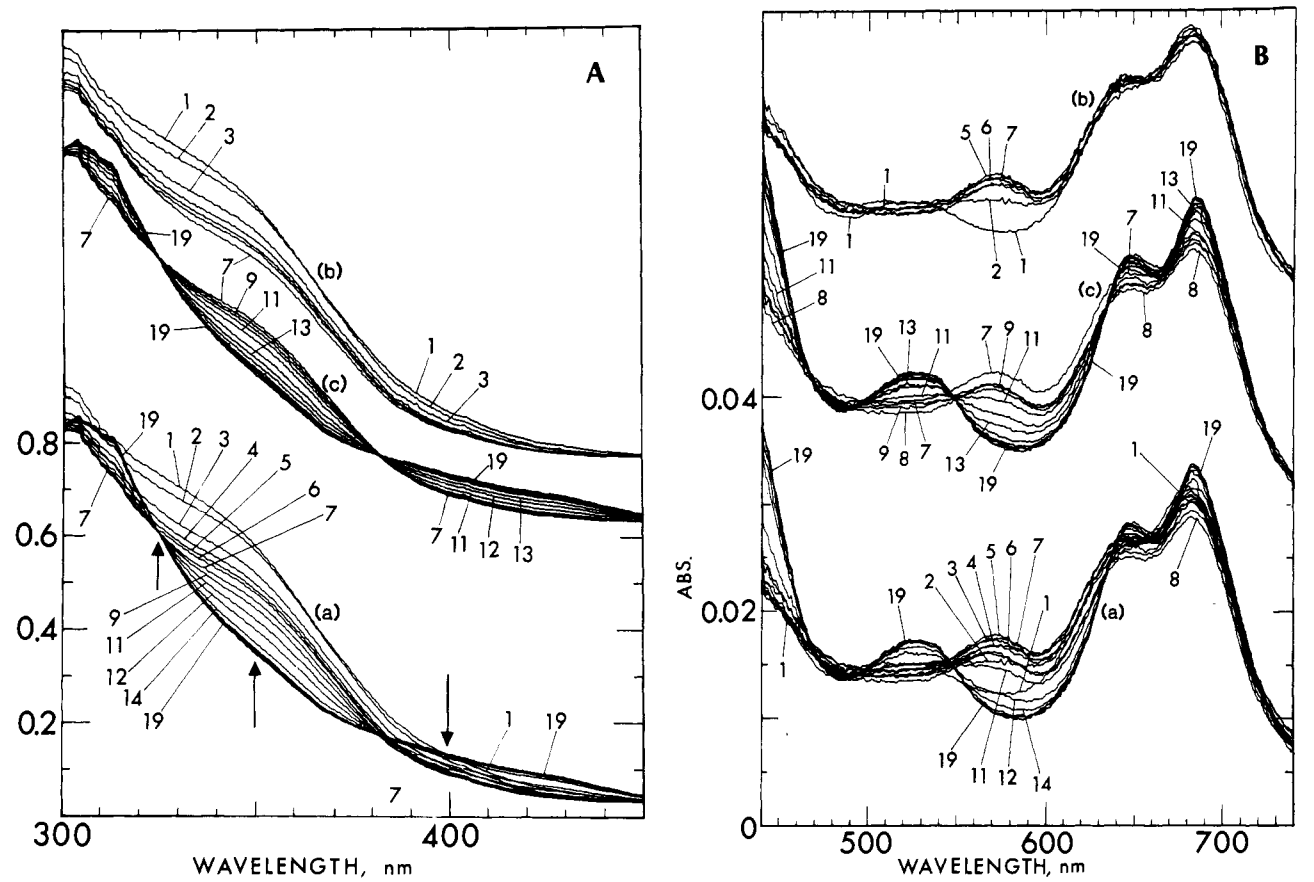

FIGURE 2: Time-resolved UV–visible spectra for the reaction of the Co(II)E(NADH) complex with NBZA. Panel A shows the wavelength region 300–450 nm. Panel B shows the region 440–740 nm. To aid in visualizing the complex spectral changes, part a of each panel presents the combined set of spectra for both phases of the reaction; parts b and c present the subsets of spectra for the fast phase (spectra 1–7) and for the slow phase (spectra 7–19) offset from each other. For clarity, the 8th, 10th, 13th, and 15th spectra have been omitted from part a of panel A, and 10th, 13, and 15th spectra have been omitted from part a of panel B. Reaction is limited to a single turnover by the inclusion of the potent inhibitor pyr in the reaction mixture. The first scan in each set was initiated approximately 5 ms after flow had stopped in the rapid-mixing stopped-flow apparatus. The repetitive scan rate was 16.48 ms/scan with additional delays introduced at longer times to space the 19 acquired scans over the 47.5-s time course of the biphasic reaction (viz., Figure 3). Conditions after mixing: (syringe 1) [Co(II)E] = 27.5 μN (79% active site substitution); (syringe 2) [NADH] = 46.8 μM, [NBZA] = 85.8 μM, [pyr] = 19 mM, 0.1 M sodium pyrophosphate–50 mM Tes buffer containing 38 mM NaCl, final pH 8.36 and 25 °C. The absorbance values refer to a 2-cm light path. The data have not been smoothed.

~313, ~400, and ~420 nm, and a maximum at ~350 nm. The shape of these spectra indicates that a charge-transfer band located at approximately 350 nm [viz., the spectra of Co(II)E and Co(II)E(NAD$^+$, TFE)] disappears in the slow phase concomitant with the appearance of the Co(II)E-(NAD–pyr) charge-transfer bands located at ~400 and ~420 nm.

The corresponding sets of difference spectra for the visible region are shown in Figure 5. Figure 5A compares the differences in the fast phase, calculated by subtracting spectrum 7 of Figure 2B from spectra 1–6. Figure 5B compares the differences in the slow phase calculated by subtracting spectrum 19 of Figure 2B from spectra 7–18. The first two difference spectra in Figure 5A show well-defined minima located at ~575 nm. Although there appear to be small minima located at ~470 and ~700 nm, the optical density changes in these regions of the spectrum are too small to be resolved under these experimental conditions.

Each difference spectrum in Figure 5B shows maxima at ~476 and ~575 nm (with a shoulder at ~615 nm) and minima at ~525, ~645, and ~684 nm. These difference spectra show the existence of apparent isosbestic points located at ~467, ~495, ~547, ~632, and perhaps ~725 nm.

The bands which form during the slow phase at 400, 420, 525, 650, and 685 nm are identical with those of the Co(II)E(NAD–pyr) complex (compare Figure 1C,D with Figure 2). The band at 575 nm which forms in the fast phase and then is seen to slowly disappear in the slow phase is remarkably similar to the 575-nm bands observed in the spectra of the ternary Co(II)E(NAD$^+$, TFE), Co(II)E(NAD$^+$, acetate) and Co(II)E(NAD$^+$, ethanol) complexes (Dietrich & Zeppezauer, 1982).

The existence of apparent isosbestic points during the slow phase (Figures 4B and 5B) provides strong evidence that the displacement of an inner-sphere-coordinated *oxy* ligand from the ternary complex is tightly coupled to the production of the pyrazole adduct. The most simple explanation for this result is that after the reduction of NBZA, NBZOH remains at the active site as the alkoxide (Dunn et al., 1979, 1982; Morris et al., 1980; Kvassman & Petterson, 1978). Upon protonation, NBZOH is released concomitantly with the production of the pyr adduct.

Saturation and Kinetic Isotope Studies. Under single turnover conditions (i.e., [pyr] $\gg$ [NBZA] > [NADH] > [Co(II)E]), the disappearance of NADH in the reaction of the Co(II)E(NADH) complex with NBZA is monophasic when measured at wavelengths corresponding to the slow phase apparent isosbestic points (324 and 380 nm, Figures 2A, 3A, and 4). The dependence of the rate of the fast phase on the concentration of substrate is shown in Figure 6. The apparent

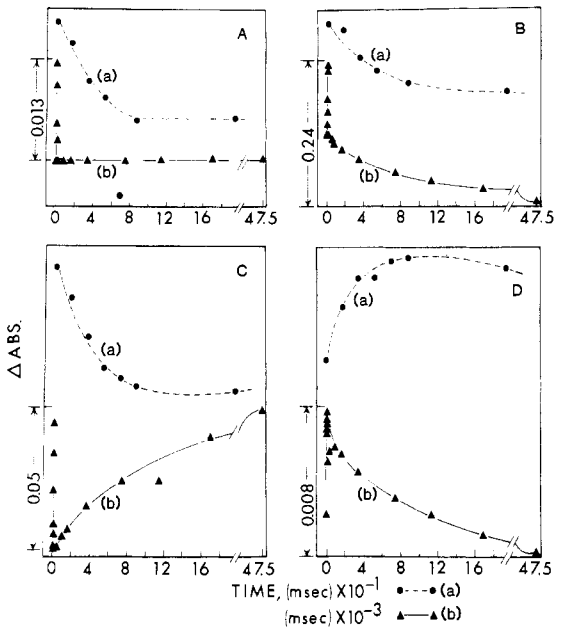

FIGURE 3: Single wavelength reaction time courses reconstructed from the rapid-scanning spectra presented in Figure 2. The "time slices" are for (A) 324, (B) 350, (C) 398, and (D) 575 nm, respectively. Note that two time scales are shown in each panel: 0–210 ms (●), and 0–21 s (▲). The final absorbance value (▲) taken from the 19th spectrum at t = 47.5 s is shown at the extreme right margin of each panel.

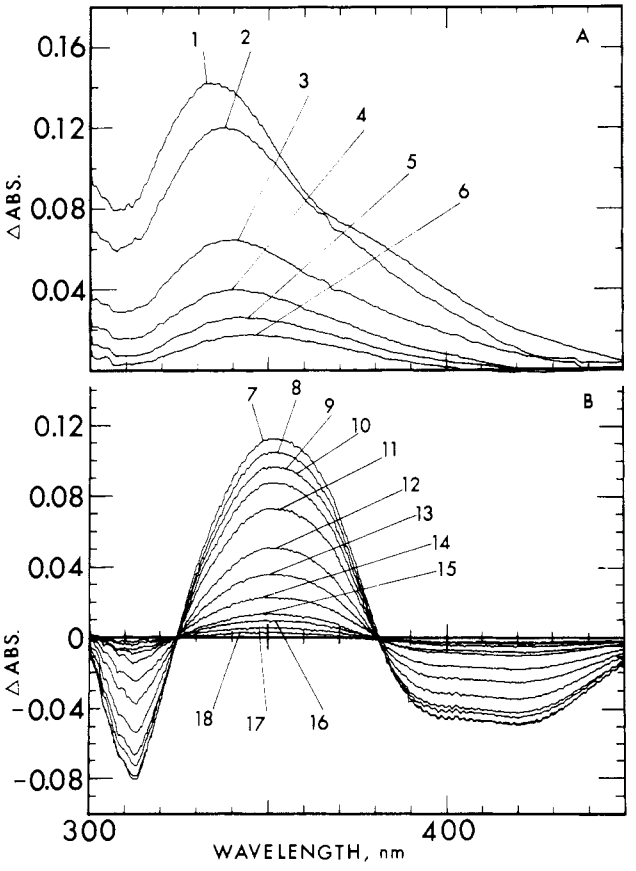

FIGURE 4: Difference spectra (numbered in chronological order), calculated from the data in Figure 2, showing the changes which occur in the 300–450-nm region for the fast (A) and slow (B) phases of the reaction. The difference spectra in (A) were calculated by subtracting spectrum 7 from spectra 1–6. The slow phase difference spectra were calculated by subtracting spectrum 19 from spectra 7–18.

first-order rate constants increase and then saturate at high concentrations of NBZA, consistent with a multstep process

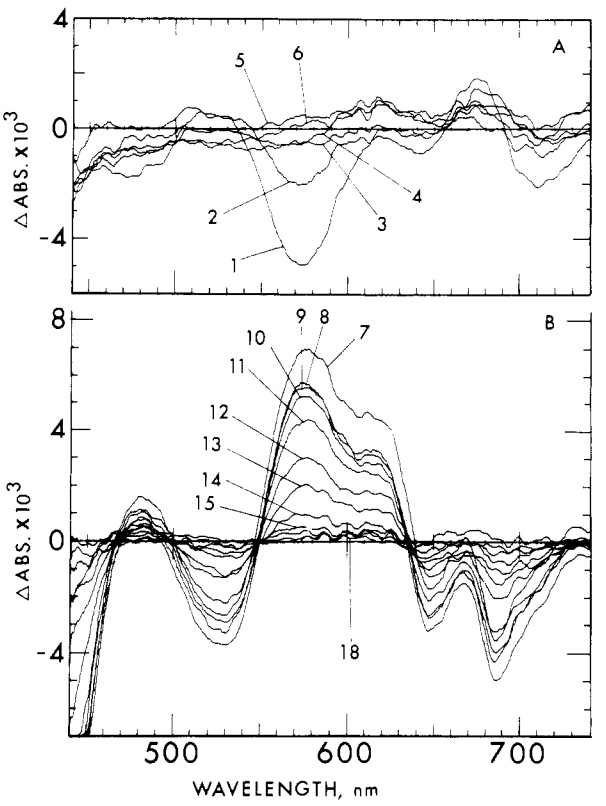

FIGURE 5: Difference spectra (numbered in chronological order), calculated from Figure 2, showing the spectral changes in the 440–740-nm region. Changes in the fast (A) and slow (B) phases were calculated as described in the legend to Figure 4. The data were smoothed to reduce high frequency noise. Smoothing was accomplished by using a second degree polynomial and point-by-point evaluation with a ~3.5-nm bandwidth and via the method of Savitzsky & Golay (1964).

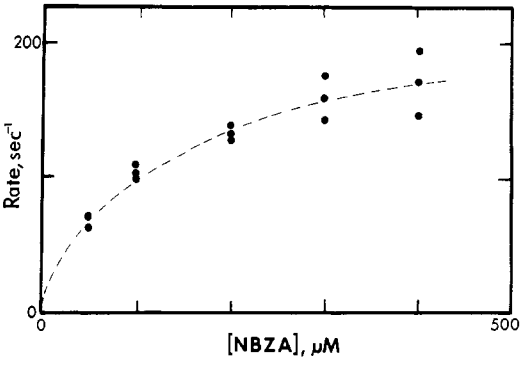

FIGURE 6: Dependence of the apparent first-order rate constant for the reaction of Co(II)E(NADH) with NBZA on the concentration of NBZA. Conditions: [Co(II)E] = 8.5 μN, [NADH] = 101 μM, 50 mM sodium pyrophosphate buffer, pH 8.75, 25.0 ± 0.2 °C. The rate constants were evaluated from single wavelength time courses measured at 379 nm by using previously described methods (Dunn et al., 1979). The dashed line is the best fit of the data to the kinetic scheme shown in eq 1 (see Discussion).

involving a rapid preequilibrium binding step prior to the chemical process which results in the observed spectral changes.

To determine if the rate-determining step for the spectral change involves hydride transfer, a parallel set of experiments were run at high substrate concentration with both NADH and NADD. Under conditions of [Co(II)E] = 16.2 μN, reduced [coenzyme] = 116 μN, [NBZA] = 294 μN, and [pyr] = 20 mM, at pH 8.80, the observed fast phase rate was found to be the same (150 ± 15 s^{-1}) for both NADD and NADH. Thus, the rate-limiting step for NADH disappearance in this

phase must occur prior to hydride transfer.

Discussion

Much investigation over the last decade has revealed that the substitution of Co(II) for Zn(II) in LADH gives species with high catalytic activity both under steady-state kinetic conditions of substrate turnover (where product coenzyme dissociation probably is rate limiting) (Drum & Vallee, 1970; Drott et al., 1974; Sytkowski & Vallee, 1975, 1976, 1978; Dietrich et al., 1979; Maret et al., 1979) and under transient kinetic conditions where hydride transfer is rate limiting (Dunn et al., 1982). Given that catalytic competence is an important criterion in enzyme modification studies, the high catalytic activity of the Co(II)E strongly implies that Co(II) substitution for Zn(II) at the active site does not radically change the intermediates and transition states along the reaction path (Dunn et al., 1982). Thus, changes in chemical mechanism inferred from comparison of the Co(II) and Zn(II) enzymes may be interpreted as reflecting the catalytic function of the metal ion in catalysis (Dunn et al., 1982).

The constraints on active site geometry imposed by protein tertiary structure favor highly similar active site geometries in native and metal-substituted enzymes. As found from X-ray crystallographic investigations of the native enzyme and of enzyme–NADH–inhibitor or –substrate complexes (Eklund et al., 1974, 1982; Cedergren-Zeppezauer et al., 1982), detailed spectral analyses of the active site substituted Co(II) enzyme (in solution) are consistent with tetrahedral liganding both for the enzyme and for ternary complexes involving coenzyme and monodentate ligands (Maret et al., 1979; Dietrich et al., 1979).

Comparison of Native and Co(II)-Substituted LADH in the Reduction of NBZA. Under single turnover conditions, the reaction of the Zn(II)E(NADH) complex with NBZA is remarkably biphasic (Dunn et al., 1979; Koerber & Dunn, 1981). Over the range of substrate concentrations accessible to study (20–200 μM), the rate of the fast phase is approximately proportional to substrate concentration. At substrate concentrations > 200 μM, the rate of the fast phase becomes too rapid for accurate measurement in our stopped-flow apparatus (k_{obsd} > 400 s^{-1}; A. Lentzner and M. F. Dunn, unpublished results). The rate of the slow phase (with k_{obsd} = 0.5 s^{-1} at pH 8.75) is nearly independent of substrate concentration. Rapid scanning UV–visible spectral studies (Koerber & Dunn, 1981) have shown that the absorbance changes *in each phase* arise from the oxidation of enzyme-bound NADH. However, only the fast phase is subject to a primary kinetic isotope effect ($k_H/k_D \simeq 2.0$) when NADD is substituted for NADH. Consequently, the rate-limiting step in the fast phase involves the transfer of hydride, whereas in the slow step some process other than hydride transfer limits the rate of oxidation of enzyme-bound NADH. Since the slow phase oxidation of NADH is concomitant with product dissociation, it has been argued that the dissociation of alcohol product from sites which reacted in the fast phase limits the slow phase rate. That is, in the slow phase NADH oxidation and product dissociation appear to be tightly coupled events (Dunn et al., 1979; Koerber & Dunn, 1981).

The reaction of NBZA with the Co(II)E(NADH) complex under single turnover conditions (in the presence of pyr) also occurs in two kinetically distinct phases (viz., Figures 2–5). At low substrate concentrations, the rate of the fast phase is proportional to the concentration of substrate, and at high substrate concentrations the rate becomes independent of the concentration of substrate with a value of 150–200 s^{-1} (Figure 6). Over the range of concentrations investigated (50–400 μM), both the rate of the slow phase and the amplitudes of the absorbance changes associated with the fast and slow phases are insensitive to the concentration of substrate. Neither phase is subject to a primary kinetic isotope effect when NADD is substituted for NADH. Both λ_{max} and band-shape analyses of the difference spectra (Figures 4 and 5) indicate that the oxidation of enzyme-bound NADH occurs during, and is completed in, the fast phase. The difference spectra unambiguously establish that the Co(II)E(NAD–pyr) adduct forms only during the slow phase of the reaction.

The 575-nm band (Figures 2 and 5) which forms during the fast phase of the reaction is modeled by the spectra of the Co(II)E(NAD^+) ternary complexes with ethanol, trifluorethanol (Dietrich & Zeppezauer, 1982), and acetate ion.[2] Indeed, the spectrum of the Co(II)E(NAD^+, TFE) complex (Figure 1D) very closely resembles the spectrum of the intermediate (trace 7, Figure 2B), while the final spectrum (trace 19, Figure 2B) is identical with the spectrum of the Co(II)-E(NAD–pyr) adduct (Figure 1). Therefore by analogy to these spectra, we propose that the 575-nm band exhibited by the intermediate is due to formation of a ternary complex involving NBZOH and NAD^+. If this assignment is correct, then the disappearance of the 575-nm band concomitant with the formation of the Co(II)E(NAD–pyr) adduct strongly indicates that the dissociation of NBZOH limits the rate of formation of the pyrazole adduct.

The rate of the slow phase (0.08 s^{-1}) is remarkably slow for the rate of dissociation of an alcohol from the ternary complex. Recent studies from our laboratories (M. Gerber, M. Zeppezauer, and M. F. Dunn, unpublished results) indicate this slow rate of dissociation originates from a slow (rate-limiting) change in conformation of the ternary complex.

Analysis of the Differences between Co(II)- and Zn(II)-Substituted LADH. Clearly, the Co(II) and Zn(II) enzymes exhibit remarkably different kinetic time courses during catalysis of the reaction between NADH and NBZA. These differences include the following: (1) The number of kinetic phases observed for the *oxidation* of enzyme-bound NADH is two for the Zn(II)E and one for the Co(II)E. (2) For the Zn(II)E, the fast phase oxidation of NADH is characterized by a hydride transfer step which is partially rate limiting, while for the Co(II)E some other step is rate limiting. (3) The events of NADH oxidation (in the slow phase) and product dissociation are tightly coupled in the Zn(II)E system, but these events are uncoupled in the Co(II)E system.

These differences are in sharp contrast to the highly similar transient kinetic properties exhibited by the Zn(II)-, Co(II)-, and Ni(II)-substituted enzymes in the reaction of *trans*-4-(dimethylamino)cinnamaldehyde (DACA) with enzyme-bound NADH (Dunn et al., 1982). In the DACA system, reaction proceeds via inner-sphere complexation of DACA, followed first by the transfer of hydride from NADH to this intermediate, then proton transfer, release of alcohol product, and formation of the E(NAD–pyr) adduct (when pyr is present). Substitution of Co(II) and Ni(II) for Zn(II) does not appear to alter either the nature of the ground states or the transition states in this system. The small changes in spectral properties, rate constants, and apparent pK_a values appear to reflect the differences in Lewis acid strengths of these metal ions. The larger effects noted for the Cd(II)E are suggested to arise from a combination of structural and electronic factors originating from the larger size of Cd(II) vis-ā-vis Ni(II), Co(II), and

[2] In work now in preparation, similar 575 nm absorbing intermediates have been detected in the reactions of the Co(II)E(NADH) complex with benzaldehyde, anisaldehyde, cyclohexanone, and acetaldehyde (M. Gerber, M. Zeppezauer, and M. F. Dunn, unpublished results).

Zn(II) (Dunn et al., 1982). However, the basic features of the DACA reaction are not substantially altered by the substitution of Cd(II) for Zn(II).

The explanation for the contrasting effects of Co(II) substitution on the catalytic properties of liver alcohol dehydrogenase measured by the NBZA and DACA reactions may reside in the substantially different reactivities of these two substrates. As measured by nucleophlic addition to carbonyls, these two substrates occupy opposite ends of the reactivity scale.

The *p*-nitro substituent conveys high reactivity to the carbonyl of NBZA, and this reactivity is manifest in a very rapid hydride transfer step, >400 s^{-1} for the Zn(II)E. The 4-dimethylamino substituent conveys a relatively low reactivity to the carbonyl of DACA, resulting in a rather slow hydride-transfer step, 7 s^{-1} for the Zn(II)E. Consequently, the more highly reactive substrate, NBZA, places more stringent kinetic demands on those enzyme transformations directly pertaining to the hydride-transfer process. Therefore any differences in mechanism arising from the substitution of Co(II) for Zn(II) are more likely to be detected with NBZA than with DACA.

The redox step in the Co(II)E-catalyzed reaction of NBZA with NADH appears to occur subsequent to the rapid preequilibrium binding of NBZA (and NADH), viz., Figure 6. The absence of a primary kinetic isotope effect upon the oxidation of NADH indicates that hydride transfer is not the rate-limiting process for the fast phase. These observations imply that in the reaction of the Co(II)E(NADH) complex with NBZA there are two steps preceding hydride transfer: the first involves formation of a ternary complex, and the second involves a process which limits the oxidation of NADH. The transformation of an outer-sphere complex to an inner-sphere complex is unlikely to be rate limiting, viz., the rapid rate of formation of the DACA intermediate with both the Co(II)E(NADH) and Zn(II)E(NADH) species ($k = 4 \times 10^7$ M^{-1} s^{-1}). Therefore, we propose that for the Co(II)E rate limitation in the redox step is due to a chemical and/or conformational relaxation of the ternary complex, $K^* = k_2/k_{-2}$ (eq 1). In the Zn(II)E system, this same process must occur

$$\text{NBZA} + \text{Co(II)E(NADH)} \underset{k_{-1}}{\overset{k_1}{\rightleftharpoons}} \text{Co(II)E(NADH, NBZA)} \underset{k_{-2}}{\overset{k_2}{\rightleftharpoons}} \text{Co(II)E(NADH, NBZA)}^* \underset{k_{-3}}{\overset{k_3}{\rightleftharpoons}} \text{Co(II)E(NAD}^+\text{, NBZOH)} \quad (1)$$

$$K_D = k_{-1}/k_1 \qquad K^* = k_2/k_{-2} \qquad K_3 = k_3/k_{-3}$$

more rapidly than hydride transfer. For example, this relaxation could involve the chemical activation of the 1,4-dihydronicotinamide moiety and/or an obligatory conformational transition in the protein. In any case, the slower rate in the Co(II)E system must have its origins in the substitution of Co(II) for Zn(II).

With the assumption that the reaction scheme described by eq 1 is correct, then the following relationships between rate and equilibrium constants must hold: Because the rate of NADH oxidation saturates without the manifestation of a kinetic isotope effect, it must be that $k_2, k_{-2} \ll k_1, k_{-1}, k_3, k_{-3}$. Given this constraint on the relative magnitudes of rate constants, then according to relaxation kinetic theory it can be shown (Bernasconi, 1976) that the dependence of the observed rate of reaction ($1/\tau$) on the concentration of NBZA is given by

$$1/\tau = k_2[S'/(K_D + S')] + k_{-2}[1/(1 + K_3)] \quad (2)$$

where $S' = [\text{Co(II)E(NADH)}] + [\text{NBZA}]$ and $K_D = k_{-1}/k_1$. When fit to eq 2 (see the dashed line in Figure 6), the data presented in Figure 6 give

$$k_2 = 217 \pm 15 \text{ s}^{-1} \quad (3)$$

$$k_{-2}/(1 + K_3) = 3.0 \pm 0.3 \text{ s}^{-1} \quad (4)$$

$$K_D = k_{-1}/k_1 = 136 \ \mu\text{M} \quad (5)$$

Since the observed time course for the disappearance of NADH is monophasic, $K^*K_3 \gg 1$. If it is assumed that the overall equilibrium constant, K_{eq}, for the reduction of NBZA (i.e., eq 6)

$$\text{NBZA} + \text{NADH} + \text{H}^+ \overset{K_{eq}}{\rightleftharpoons} \text{NBZOH} + \text{NAD}^+ \quad (6)$$

is dominated by the redox step, K_3, then at pH 8.75 where $K_{eq}[H^+] = 940$ (Dunn et al., 1979), K_3 must be $\gg 1$. It then follows from eq 4 that

$$k_{-2} = 3(1 + K_3) \gg 1 \quad (7)$$

If K_3 is the same order of magnitude as $K_{eq}[H^+]$ (i.e., 10^2–10^3), then $k_{-2} \geq k_2$ and $K^* \leq 1$. The assignment of a value for $K_3 \gg 1$ is in accord with the nature of the spectral changes observed in Figures 2–5 where it is clear that the interconversion of ternary complexes greatly favors formation of Co(II)E(NAD^+, NBZOH).

Replacement of Zn(II) by Co(II) undoubtedly changes the specific rate constants for certain steps in the mechanism. In the DACA system, the increased Lewis acid strength of Co(II) in comparison to Zn(II) brings about an increase in the rate of hydride transfer along with a corresponding reduction of both ligand dissociation rate constants and the apparent pK_a values of coordinated ligands (Dunn et al., 1982). It is likely that the 6-fold slower apparent rate of NBZOH dissociation from the Co(II)E(NAD^+, NBZOH) complex is a consequence of the stronger Lewis acid strength of Co(II). The pH-dependent rate of alcohol product dissociation may be described by an apparent protonic ionization (Morris et al., 1980; Dunn et al., 1982). In the DACA system, the pK_{app} for this process is lowered by ~3-fold upon substitution of Co(II) for Zn(II) at the active site (Dunn et al., 1982). If the corresponding pK_{app} also is lowered upon substitution of Co(II) for Zn(II) in the Co(II)–enzyme–NBZA system, a decrease of severalfold in the NBZOH dissociation rate would be expected.

It has been postulated that the biphasicity of NADH oxidation under single turnover conditions is a consequence of site catalytic nonequivalence (i.e., the LADH reaction involves half-of-the sites reactivity; Bernhard et al., 1970; Dunn et al., 1979; Koerber & Dunn, 1981). Alternatively, noncooperative explanations involving (fortuitous) combinations of rate and equilibrium constants and spectral changes for the process of substrate and product binding and for the interconversion of ternary complexes have been proposed by others (viz., Kvassman & Pettersson, 1976; Wiedig et al., 1977; Andersson & Pettersson, 1982; W. Bloch, private communication).

The site nonequivalence model in essence proposes the existence of at least two conformational forms of the subunits with different catalytic activities in asymmetric dimers, viz., Scheme I. If the interconversions of the asymmetric and symmetric forms are slow relative to the redox process, then the oxidation of bound NADH will be biphasic and (to a first approximation) the magnitude of K_1 will determine the distribution of active and inactive subunits ($K_2 = 1$ by definition) and consequently the amount of NADH oxidized in the fast phase. The rate of the slow phase oxidation of NADH will be determined by the process which limits the interconversion

Scheme I[a]

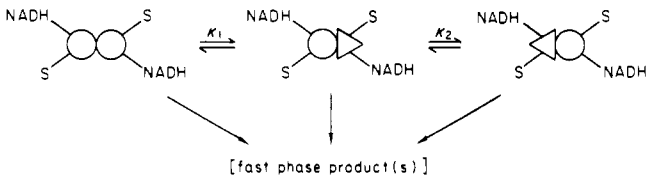

[a] Circles designate highly catalytically active subunits, and triangles designate inactive subunits.

Scheme II[a]

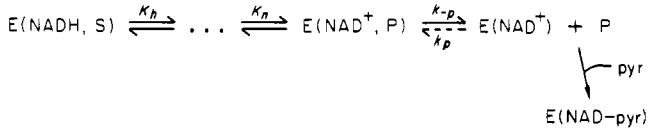

[a] K_h through K_n designate the equilibrium constants for the individual steps involved in the interconversion of ternary complexes, and k_p and k_{-p} are the specific rate constants for product binding and dissociation.

of active and inactive forms (i.e., the interconversion of circles and triangles). If the free energy change for the interconversion of ternary complexes favors E(NAD$^+$, P), then the relative amplitude of the fast phase, $A_{fast}/(A_{fast} + A_{slow})$, could (depending upon the value of K_1) range from 0.5 to 1.0. If the magnitude of K_1 depends upon the chemical/physical structure of the substrate, then the amplitude ratio will vary with substrate structure.

The alternative explanations involving fortuitous combinations of rate and equilibrium constants proposed to explain the biphasicity are summarized in (generalized) Scheme II. Under conditions where k_{-p} is slow relative to the interconversion of ternary complexes, k_p is negligible, and the product of equilibrium constants, $\prod_{n=h}^{n}(K_h) \simeq 1$, the single turnover reaction will be biphasic with $A_{fast}/(A_{fast} + A_{slow}) \simeq 0.5$. Biphasicity in this mechanism arises as a consequence of the rapid equilibration of E(NADH, S) and E(NAD$^+$, P) followed by a relatively slow rate of k_{-p} which limits the conversion of E(NAD$^+$, P) to the E(NAD–pyr) complex.

Irrespective of the microscopic origins of the biphasic oxidation of NADH, it is clear that the site-specific substitution of Co(II) for Zn(II) abolishes this biphasicity. With reference to Schemes I and II, substitution of Co(II) must either shift K_1 to greatly favor the symmetric species (Scheme I) or, alternatively, shift $\prod_{n=h}^{n}(K_h)$ to a value much greater than 1 (Scheme II). In either case, the substitution of Co(II) for Zn(II) must bring about significant changes in ground states and transition states in the mechanism of NBZA reduction.

Registry No. NADH, 58-68-4; NAD, 53-84-9; alcohol dehydrogenase, 9031-72-5; *p*-nitrobenzaldehyde, 555-16-8; *p*-nitrobenzyl alcohol, 619-73-8; isobutyramide, 563-83-7; 2,2,2-trifluoroethanol, 75-89-8; pyrazole, 288-13-1.

References

Andersson, P., & Pettersson, G. (1982) *Eur. J. Biochem. 122*, 559–568.

Bernasconi, C. F. (1976) in *Relaxation Kinetics*, Academic Press, New York.

Bernhard, S. A., Dunn, M. F., Luisi, P. L., & Schack, P. (1970) *Biochemistry 9*, 185–192.

Cedergren-Zeppezauer, E., Samama, J.-P., & Eklund, H. (1982) *Biochemistry 21*, 4895–4908.

Dietrich, H., & Zeppezauer, M. (1982) *J. Inorg. Biochem. 17*, 227–235.

Dietrich, H., Maret, W., Wallén, L., & Zeppezauer, M. (1979) *Eur. J. Biochem. 100*, 267–270.

Drott, H. R., Santiago, D., & Shore, J. D. (1974) *FEBS Lett. 39*, 21–23.

Drum, D. E., & Vallee, B. L. (1970) *Biochemistry 9*, 4078–4086.

Dunn, M. F., & Hutchison, S. J. (1973) *Biochemistry 12*, 4882–4892.

Dunn, M. F., Bernhard, S. A., Anderson, D., Copeland, A., Morris, R. G., & Roque, J.-P. (1979) *Biochemistry 18*, 2346–2354.

Dunn, M. F., Dietrich, H., MacGibbon, A. K. H., Koerber, S. C., & Zeppezauer, M. (1982) *Biochemistry 21*, 354–363.

Eklund, H., Nordström, B., Zeppezauer, E., Söderlund, G., Ohlsson, I., Boiwe, T., & Brändén, C.-I. (1974) *FEBS Lett. 44*, 200–204.

Eklund, H., Samama, J.-P., & Wallén, L. (1982) *Biochemistry 21*, 4858–4866.

Koerber, S. C. (1981) Doctoral Dissertation, University of California, Riverside.

Koerber, S. C., & Dunn, M. F. (1981) *Biochimie 63*, 97–102.

Kvassman, J., & Pettersson, G. (1976) *Eur. J. Biochem. 69*, 279–287.

Kvassman, J., & Pettersson, G. (1978) *Eur. J. Biochem. 87*, 417–427.

Maret, W., Andersson, I., Dietrich, H., Schneider-Bernlöhr, H., Einarsson, R., & Zeppezauer, M. (1979) *Eur. J. Biochem. 98*, 501–512.

McFarland, J. T., & Bernhard, S. A. (1972) *Biochemistry 11*, 1486–1493.

Morris, R. G., Saliman, G., & Dunn, M. F. (1980) *Biochemistry 19*, 725–731.

Rafter, G. W., & Colwick, S. P. (1957) *Methods Enzymol. 3*, 887–888.

Savitzsky, A., & Golay, M. J. E. (1964) *Anal. Chem. 36*, 1627–1639.

Shore, J. D., & Santiago, D. (1975) *J. Biol. Chem. 250*, 2008–2012.

Silverstein, E. (1965) *Anal. Biochem. 12*, 199–212.

Sloan, D. L., Young, J. M., & Mildvan, A. S. (1975) *Biochemistry 14*, 1998–2008.

Sund, H., & Theorell, H. (1963) *Enzymes, 2nd Ed. 7*, 25–83.

Sytkowski, A. J., & Vallee, B. L. (1975) *Biochem. Biophys. Res. Commun. 67*, 1488–1493.

Sytkowski, A. J., & Vallee, B. L. (1976) *Proc. Natl. Acad. Sci. U.S.A. 73*, 344–348.

Sytkowski, A. J., & Vallee, B. L. (1978) *Biochemistry 17*, 2850–2857.

Tilander, B., Strandberg, B., & Fridborg, K. (1965) *J. Mol. Biol. 12*, 740–760.

Weidig, C. F., Halvorson, H. R., & Shore, J. D. (1977) *Biochemistry 16*, 2916–2922.